Journal of Ecological Engineering, 2026, 27(1), 40–51 https://doi.org/10.12911/22998993/208858 ISSN 2299–8993, License CC-BY 4.0

Effect of a green corrosion inhibitor on the chemical composition and surface morphology of N80 steel in carbon dioxide-saturated brine at elevated temperature

Gordana Bilić¹, Ewa Knapik^{1,2}, Przemysław Toczek^{1,2}, Katarina Žbulj¹, Igor Medved¹

- ¹ Faculty of Mining, Geology and Petroleum Engineering, University of Zagreb, 10000 Zagreb, Croatia
- ² Faculty of Drilling, Oil and Gas, AGH University of Krakow, al. Mickiewicza 30, 30-059 Krakow, Poland
- * Corresponding author's e-mail: eknapik@agh.edu.pl

ABSTRACT

The decarbonization of European industry will require large-scale underground CO₂ storage. To ensure the long-term safety of storage sites, it is essential to maintain the integrity of both the geological formation and the surface infrastructure. A critical component exposed to elevated risk are production pipelines and tubing, which operate under highly corrosive conditions – typically involving CO₂-saturated brine at elevated temperatures constitute critical components exposed to elevated risk. To mitigate corrosion, chemical inhibitors are commonly injected into the system. In line with sustainability goals, the use of environmentally friendly, or "green," corrosion inhibitors is recommended. Among many green inhibitors, citrus extracts are particularly popular. In this study, the effect of an alcoholic extract from mandarin peels on the surface of N60 steel was investigated in a 3.5% NaCl environment saturated with CO₂ at 60 °C. Infrared spectroscopy (IR) was used to identify active compounds in the extract and assess the chemical interactions between the steel and the brine, while surface morphology was evaluated using scanning electron microscopy (SEM). The results showed that the inhibitor remained present on the steel surface even at elevated temperatures, whereas the steel surface exhibited less degradation and was more homogeneous. The elemental composition of steel determined by SEM-EDS confirms the presence of a protective layer: the Fe content increases from 66.66% (sample without inhibitor) to 82.50% (with inhibitor), which indicates that the Fe dissolution rate decreases in the presence of the inhibitor.

Keywords: corrosion, inhibitor, CO₂-saturated brine, mandarin peel extract.

INTRODUCTION

In the face of a deepening climate crisis, the European Union is pursuing an increasingly ambitious climate policy aimed at reducing greenhouse gas emissions and achieving climate neutrality by 2050 (Bouckaert et al., 2021). A key instrument of this strategy is the EU Emissions Trading System (EU ETS), the importance of which continues to grow alongside the tightening of environmental standards. In recent years, a dynamic increase in carbon emission allowance prices has been witnessed, which carries significant consequences for both industry and consumers (Wu, 2025). Emission allowance prices have become

not only an indicator of climate policy but also a major economic factor, influencing energy costs, production expenses, and the competitiveness of the European economy. The EU ETS has proven to be an effective tool in reducing GHG emissions – between 2005 and 2022, it contributed to a 42.8% decrease in CO₂ emissions (Klimko and Hasprová, 2025). However, it also raises significant concerns in certain sectors of the economy, particularly regarding rising operational costs and the potential relocation of business activities to countries with less stringent environmental regulations (Błażejowska et al., 2024; Vaca-Cabrero et al., 2024). Companies are adopting various decarbonization strategies in response to climate

Received: 2025.07.20 Accepted: 2025.09.31

Published: 2025.11.25

policies and stakeholder expectations. These include improving energy efficiency, switching to renewable energy sources and renewable fuels (Litvak and Litvak, 2020; Łukomska et al., 2024), electrifying industrial processes (Masuku et al., 2024), development of hydrogen economy (Stobnicki and Gallas, 2022), redesigning products and supply chains. In the sectors where emissions are unavoidable, such as in gas-fired power plants, the implementation of carbon capture and storage (CCS) technology is essential. The Net-Zero Industry Act sets a minimum target of 50 million tonnes of CO₂ injection capacity per year by 2030 in Europe (Talus and Maddahi, 2024) and now every European country is carefully assessing its CO₂ storage capacity. The available options for underground CO2 storage include deep saline aquifers, depleted oil and gas reservoirs, and unmineable coal seams (Bashir et al., 2024). Poland, the third-largest greenhouse gas emitter in the EU, releases around 380 Mt CO2 annually, making CCS a particularly cost-effective mitigation option (Climate Action Progress Report 2023, 2023; Kopacz et al., 2024). With an estimated storage capacity of about 15 Gt in saline aguifers and depleted reservoirs (Dziadzio, 2023) - Poland could theoretically store several centuries' worth of its industrial CO₂ emissions. Croatia is actively pursuing a strategy to become a leader in CCS within the Adriatic region with the storage potential of about 4 Gt (Saftić et al., 2024; Vulin et al., 2023).

CCS raises concerns regarding the safety and integrity of storage sites (Shuter et al., 2011), especially considering the demanding operating conditions: elevated temperatures of around 60°C, high pressures reaching several tens of MPa, and significant water salinity. Table 1 presents the operating conditions of typical CO₂ storage sites.

Such conditions promote the corrosive degradation of casing pipes and cement. Carbon dioxide, when dissolved in water, forms carbonic acid, H₂CO₃ (Al-Janabi, 2020). The general reaction equation with iron can be written as:

Fe
$$+2H_2CO_3 \rightarrow Fe^{2+} + +2HCO_3^- + H_2$$
 (1)

The mechanism of anodic dissolution depends on the pH value and is typically written as:

$$Fe \rightarrow Fe^{2+} + 2e^{-}$$
 (2)

The cathodic process involves the direct reduction of bicarbonate ions and oxygen:

$$2HCO_3^- + 2e^- \rightarrow 2CO_3^{2-} + H_2$$
 (3)

$$0_2 + 2H_2O + 4e^- \rightarrow 4OH^-$$
 (4)

The solubility of carbon dioxide in water generally follows Henry's law: the higher the pressure in the system, the greater the solubility of CO₂. Temperature has an even more significant effect on the process - its decrease leads to an increase in gas solubility. The influence of these parameters on the corrosion rate is described by equation:

$$log R = 7.96 - \frac{2320}{T + 273} - \frac{5.55T}{1000} + 0.67 log(p_{CO_2})$$
(5)

where: R – the corrosion rate (mm/yr), T – temperature (°C), p_{co2} – the partial pressure of CO_2 .

The corrosion rate in carbonate solutions is accelerated by the presence of dissolved H₂S. At low concentrations of hydrogen sulfide, a protective sulfide layer may form; however, its overall presence lowers the pH of the environment, which in turn accelerates anodic reactions. On the basis of the partial pressures of CO₂ and H₂S in the system, corrosion severity classes have been established for oil and gas wells (Stachowicz, 2010) (Table 2).

To mitigate corrosion, it is necessary to regularly inject corrosion inhibitors, especially in the cases where processes like EOR-WAG (Enhanced Oil Recovery - Water-Alternating-Gas) are implemented, involving the alternating injection of CO2 and water into the reservoir. To reduce the use of chemicals (usually amines, imidazolines and Schiff bases), there is a growing trend toward the application of green corrosion inhibitors (Shang and Zhu, 2021). So far, various naturally derived substances, usually oils and extracts obtained from agro-industrial waste, have been tested as corrosion inhibitors including coffee bagasse oil (Gomez-Guzman et al., 2019), dandelion-root extract (Žbulj et al., 2022), passion fruit seed oil microemulsion (Souza et al., 2020), olive leaf extract (Pustaj et al., 2016), citrus peels extracts (Zhang and Zhao, 2018), extracts from pomegranate, lemon balm leaves, grape pomace, burdock root and liquorice root (Žbulj et al., 2021). Among the tested inhibitors, citrus extracts

| Zhang et al., 2022) | | | | | | |
|----------------------------|------------|-----------------------------|----------------------------|--------------------------|------------|--|
| CCS project | Water type | Total dissolved solids, g/L | Reservoir pressure, MPa | Reservoir temperature, C | Depth, m | |
| Sleipner, Norway NaCl | | 35 | 10 | 32 | 800–1000 | |
| Rousse (Lacq), France NaCl | | 2–40 | currently about 9 | up to 150 | 4500 | |
| Gorgon, Australia | NaCl | 10–35 | up to 20 | 70 | about 2000 | |
| Kotzin Gormany | NaCl | 200 | 6.7 | 2/1 20 | 620, 650 | |

Table 1. Water chemistry in typical CCS projects (Ivanowa, 2013; Prinet et al., 2013; Weijermars, 2024; Zhang et al., 2022)

Table 2. Effect of partial pressures of CO₂ and H₂S on corrosion rate

| Expected | Conditions | | |
|----------------|------------------------|------------------------|--|
| corrosion rate | pH ₂ S[MPa] | pCO ₂ [MPa] | |
| Very high | > 2.5 | >0.2 | |
| High | < 2.5 | ≥ 0.2 | |
| Medium | > 2.5 | < 0.2 | |
| Below average | < 2.5 | < 0.2 | |
| Low | Other | | |

(oranges, tangerines, lemons) deserve special attention, as these fruits are widely cultivated and easily accessible worldwide. Citrus peels contain pectin, alkaloids, monoterpenes, carotenoids (β-cryptoxanthin and lutein), hesperidin, polyphenols, and vitamin C (Sanli et al., 2025) and most heterocyclic compounds with lone pairs of electrons on sulfur (S), nitrogen (N), as well as oxygen (O) atoms have a tendency to adsorb onto and interact with metal surfaces. Numerous electrochemical and gravimetric studies confirm the effectiveness of citrus extracts. The study by Zhang and Zhao (2018) shows that an orange peel extract exhibits high inhibition efficiencies of 97.6% and 73.1% at a concentration of 1000 mg/L in CO2 and CO2/H2S brine solutions, respectively. The work of (Elazabawy et al., 2023) reported that an orange peel extract functions as a mixed-type corrosion inhibitor for carbon steel in real formation water, with a recorded inhibition rate of 90.13% at a dosage of 2.5% and ambient temperature (25 °C). Wang et al. (2017) studied the inhibition properties of tangerine peel extract on J55 steel in CO₂-saturated 3.5 wt. % NaCl solution. Their electrochemical measurements show that the extract at a concentration of 4% vol. has the inhibition efficiency of about 83%, but it decreases with temperature.

Although electrochemical and gravimetric measurements provide a good quantitative description of corrosion, an in-depth surface

analysis is necessary to explain the mechanism of the process. In this study, attention was focused on the surface aspects, specifically a detailed examination of the composition and morphology of steel surfaces corroded in CO₂-saturated brine in the presence of mandarin peel extract. Detailed SEM-EDS analyses enabled the identification of corrosion products and confirmed the good adsorption properties of the active components of the extract on the steel surface.

MATERIAL AND METHODS

Materials

Mandarins were purchased at a local market in Zagreb. The fruit pulp was mechanically separated from the peels, which were then dried at 40 °C for seven days. The dried peels were ground using a blender and sieved through a 0.1 mm mesh. The resulting powder was extracted with ethanol under the following conditions: 10 g of powder per 50 mL of ethanol at 40 °C in an ultrasonic bath. The mixture was filtered using a paper filter, and the obtained extract was used in subsequent experiments as a corrosion inhibitor.

A synthetic brine was used as the corrosive medium, prepared by dissolving 30.0 g of NaCl, 0.1 g of NaHCO₃, and 0.1 g of CaCO₃ in 1 L of distilled water. During the corrosion tests, the brine was saturated with CO₂ gas (99.5% purity) supplied by Air Liquide.

Methods

A steel sample, circular in cross section, with an area of 1 cm², made of N80 steel, was thoroughly polished with sandpaper, washed with distilled water and degreased with ethanol. It was then placed in a closed glass container filled with brine (or brine containing 1 wt.% mandarin peel extract), saturated with CO₂ at a constant gas flow

rate of approximately 100 mL/min, and maintained for 24 hours at 60 °C. After exposure to the corrosive medium, the plate was rinsed several times with distilled water and dried in an oven for 30 minutes at 40 °C temperature. The total duration of corrosion testing is typically determined based on the specific objectives of the study, the nature of the tested material, the applied methodology, and the evaluation criteria for corrosion-related changes. In the literature, different researchers adopt various exposure times, including 24, 72, 96, 240, 480, and 720 hours, depending on the context and aims of their investigations (Surowska, 2002). For example, Okafor et al. (2010) examined the surface morphology of N80 carbon steel specimens immersed in CO₂-saturated 3% NaCl solutions containing imidazoline-based inhibitors after just 2 hours of exposure. Zhang and Zhao (2018) on the other hand, tested the effectiveness of orange peel extract at 60 °C for 24 hours, while Wang et al. (2017) investigated a gemini corrosion inhibitor on N80 steel at 70 °C for 72 hours. Since there is no universally accepted testing methodology, a standard exposure time of 24 hours was selected in the conducted study.

The functional groups present in the extracts were identified using Fourier transform infrared (FTIR) spectroscopy with an Avatar 360 FT-IR spectrometer (Thermo Nicolet, Thermo Fisher Scientific, Waltham, MA, USA). Spectra were acquired in transmission mode using KBr pellets in the range of 500–4000 cm⁻¹. The chemical composition of the products deposited on the surface of steel plates after 24 hours of exposure to the corrosive medium (with and without the corrosion inhibitor) was evaluated based on the IR spectra recorded using a Nicolet iS5 FTIR

spectrometer equipped with an iD7 attenuated total reflection (ATR) accessory (Thermo Fisher Scientific, Waltham, MA, USA). All measurements were performed in triplicate, with 32 scans per spectrum.

The surface morphology of steel samples was evaluated with Apreo 2S low vac high-resolution scanning electron microscope from ThermoFisher Scientific (Waltham, MA, USA) operating at the accelerating voltage of 15 kV with the ETD detector. The elemental composition of surface deposits was assessed with the Octane Elite EDX detector operated with APEXTM Advanced 2022 software.

RESULTS AND DISCUSSION

IR spectra of pure mandarin peel extract and steel surface after corrosion tests

From the point of view of corrosion inhibition it is important to identify the functional groups able to interact with the steel surface and form a protective layer. Figure 1 shows the IR spectra of the ethanolic extracts from mandarin peels. The IR spectrum of mandarin peel extract is typical for all citrus-based extracts. All major absorption bands were identified in Table 3.

IR spectra provide an insight into the surface chemistry during the corrosion process. Figure 2 shows the IR spectra of the N80 carbon steel surface after 24 h of exposure to brine solution saturated with CO₂ in the presence and absence of the inhibitor at 60 °C.

The spectra of pure steel surface is smooth, without any strong absorption bands. The

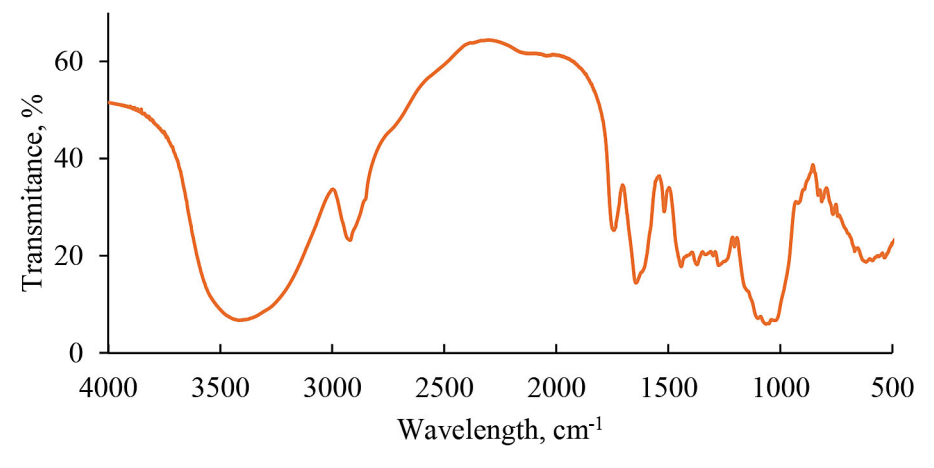


Figure 1. IR spectra of the extract obtained from mandarin peels dried at 40 °C

| Table 3. Characteristic absorption bands in the IR spectra of the mandarin peel extract (Elazabawy et al., 2023; |
|--|
| Palumbo et al., 2019) |

| Wavelength, cm ⁻¹ | Assignment |
|------------------------------|--|
| 3600–3200 | O-H stretching (carbohydrates, alcohols, phenols and water) |
| 2915 | C-H stretching (aliphatic chains (-CH ₂ - and -CH ₃)) |
| 1730 | C=O (carbonyl group in ketones and esters) |
| 1640 | C=C (alkenes and aromatic rings) |
| 1517 | –NH– (imino group) |
| 1440 | C–H bending (aliphatic chains) |
| 1370 | C–H rocking (in methyl group) |
| 1270 | C-O stretching in carboxylic acids |
| 1143, 1050, 1015 | symmetrical and asymmetrical ring breathing vibrations of C-C-O and C-O-C |
| 912, 837, 772 | associated with the glucoside (1–4) linkage and the (1–6) linkage |

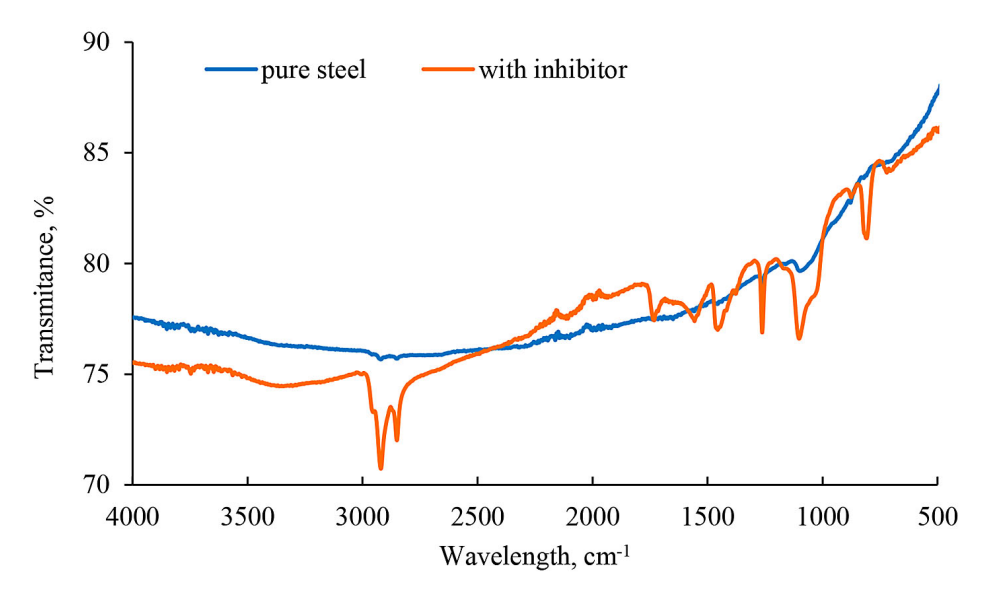


Figure 2. IR spectra of the N80 carbon steel surface after 24 h of exposure to brine solution saturated with CO₂ in the presence and absence of the inhibitor at 60 °C

metal-oxygen bond peaks related to the corrosion products appear usually in the range of 800-400 cm⁻¹ (Pasieczna-Patkowska et al., 2025) and are not strong. The IR spectra of the steel surface after 24 h of exposure to brine solution saturated with CO, in the presence of the inhibitor confirms the presence of organic functional groups on the steel surface. What is more, these are quite intense bands, which indicates that even at elevated temperatures the organics are permanently bound to the metal surface. The visible peaks at 2918 and 2850 are a result of C-H stretching and any hydrocarbon chains are beneficial for corrosion inhibition. Although the carbon skeleton itself does not react with steel, it acts as a protective shield. The absorption bands characteristic of oxygen-based organic

compounds in the range of 1700–1100 cm⁻¹ suggest interactions between the steel surface and lone electron pairs on oxygen atoms.

Surface morphology

The surface morphologies of the steel samples immersed in CO₂-saturated brine, with and without of 1 vol.% mandarin peel extract, at 60 °C after 24 h of exposure to tested electrolytes are shown in Figure 3. The SEM images of pure steel (Figure 3a–b) reveal a specimen with a smooth surface morphology. No visible inclusions are detected. However, numerous linear scratches can be observed across the surface, which are attributed to the mechanical polishing process. These polishing marks are randomly oriented and vary

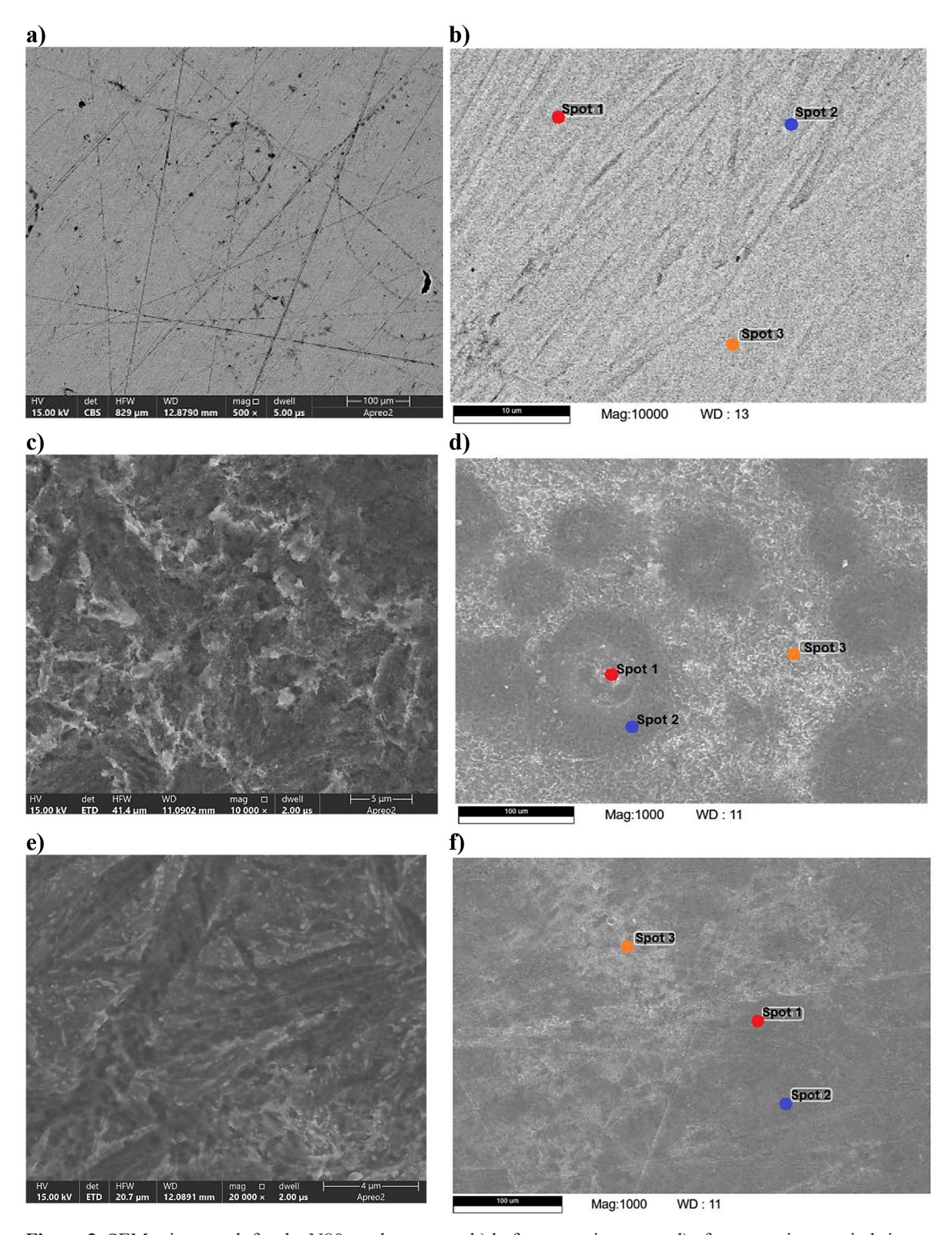


Figure 3. SEM micrograph for the N80 steel coupon a-b) before experiments, c-d) after corrosion test in brine at 60 °C, e-f) after corrosion test in brine with 1 % vol. of the MP extract at 60 °C

in length and intensity, confirming that the surface was prepared prior to further analysis.

The SEM image of the steel surface exposed to CO₂-saturated brine without inhibitor reveals

significant surface degradation (Figure 3c–d). At low magnification (Figure 3d), the surface appears highly heterogeneous, characterized by clusters of dark patches randomly distributed

across the sample. Higher magnification (Figure 3c) reveals a severely damaged surface with an irregular and rough morphology. Numerous deep grooves and cracks are visible, along with sharp, bushy corrosion products lacking a distinct crystalline structure. These features indicate intensive localized corrosion and surface breakdown due to the absence of protective inhibitor action. The steel surface in the presence of the corrosion inhibitor (Figure 3 e-f) exhibits a relatively smooth and protected morphology. Although some depressions are visible, they are wide and shallow, corresponding to polishing scratches rather than corrosion pits. The surface appears mostly uniform, with local irregularities that may indicate the adsorption or accumulation of inhibitor molecules on the steel substrate.

N80 steel is one of the most commonly used types of steel in the oil industry. Since casing and production pipes operate under extreme conditions - such as brines, acid gases, and high pressures and temperatures - their corrosion resistance has been extensively tested. The reported corrosion rate determined from weight loss measurements in CO2-saturated brine at atmospheric pressure and 60 °C was 0.076 mm/year, and it began to increase with rising temperature, exceeding 0.22 mm/year at 95 °C (Ma and Gu, 2024). A further increase in temperature (and consequently pressure up to 0.2 MPa in the test setup) within the range of 110 to 160 °C resulted in a rapid escalation of the corrosion rate from approximately 0.25 to 0.85 mm/year. Adding a tangerine (mandarin) peel extract to CO2-saturated brine at inhibitor concentrations ranging from 100 to 800 mg/L reduces the corrosion rate by 47.1–86.4% (Wang et al., 2017). The efficiency of the MP extract is slightly better than that of other green inhibitors and comparable to some commercial products, as illustrated in Table 4.

Surface elemental composition

The elemental composition at the locations marked with colored dots in Figure 3b, d, and f was determined using the SEM-EDS method. The obtained spectra are shown in Figure 4 a-b and results are summarized in Table 5.

The EDS spectrum of steel after corrosion tests without inhibitor shows more peaks and a greater variety of elements exposed on the surface, indicating a heterogeneous composition of corrosion products. In contrast, the spectrum of the steel coated with a corrosion inhibitor reveals mainly iron peaks — high Fe content on the steel surface means that the metal remains largely undissolved.

The points for SEM-EDS analysis, marked with colored dots in Figure 3b, d, and f, were selected from different regions of the sample (both bright and dark areas) to evaluate the degree of surface heterogeneity. A comparison of the elemental composition measured at spots 2 and 3 for steel without corrosion inhibitor reveals significant differences – the carbon content is 3.44% and 19.12%, respectively – indicating a non-uniform distribution of corrosion products on the surface. The average carbon content on steel

| Table 4. Comparison of the efficiency of selected green and commercial corro | osion inhibitors for N80 steel |
|--|--------------------------------|
| in CO ₂ -saturated brine | |

| Corrosion inhibitor | Experimental details | Inhibition efficiency, % | Reference | |
|------------------------------------|--|--------------------------|------------------------|--|
| Tangerine (mandarin) peel extract | At optimal concentration of 600 mg/L | 86.9 | (Wang et al., 2017) | |
| Guar gum | At concentration of 500 mg/L and 45 °C in CO ₂ -saturated 0.5 M KCl, obtained from weight loss measurements | 40.74 | (Palumbo et al., 2019) | |
| Olive leaf extract | 300 ppm of extract, obtained from polarization method, at 65 °C | 90.1 | (Pustaj et al., 2017) | |
| Pomelo peel extract | 400 mg/L, at 60 °C | 75 | (Sun et al., 2017) | |
| B-N-butyl amino propionic acid | With 100 ppm of inhibitor at 60 °C | 93.90% | (Wang et al., 2024) | |
| Furfuryl mercaptan (food flavor) | With 10 ppm of inhibitor at 60 °C | 96.9 | (Wang et al., 2023) | |
| Difurfuryl disulfide (food flavor) | With 10 ppm of inhibitor at 60 °C | 99.1 | (Wang et al., 2023) | |
| Imidazoline-based salt | At 25 °C, inhibitor concentration of 400 mg/L, using polarization method | 93.8 | (Okafor et al., 2010) | |
| Mannich base (MBT) | At 70 °C and 400 mg/L of MBT | 90.4 | (Tang et al., 2019) | |
| CX-1 Chinese commercial product | With 60 ppm of inhibitor at 80 °C | ca. 67 | (Ma and Gu, 2024) | |

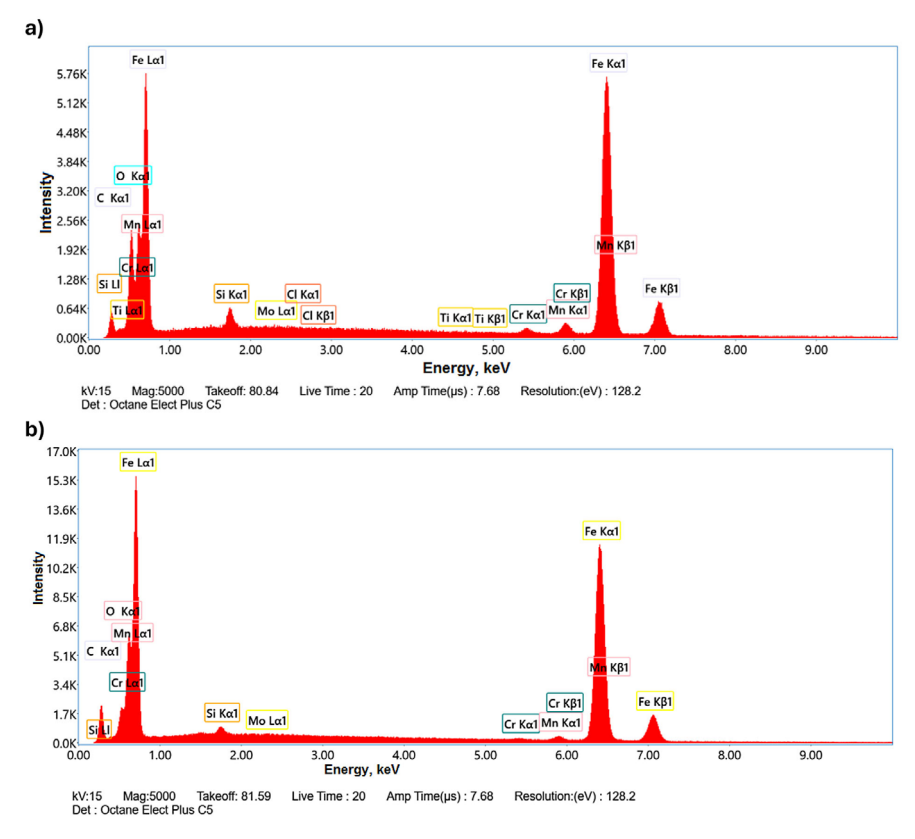


Figure 4. EDS spectra of corrosion products on the N80 steel sample a) without corrosion inhibitor, b) in the presence of the mandarin peel extract

Table 5. Elemental composition of corrosion products

| | Elemental composition by weight, % | | | | | |
|---------|---|--------|--------|--|--------|--------|
| Element | After corrosion at 60 °C without the MP extract | | | After corrosion at 60 °C with the MP extract | | |
| | Spot 1 | Spot 2 | Spot 3 | Spot 1 | Spot 2 | Spot 3 |
| Fe | 53.04 | 78.94 | 67.99 | 81.94 | 78.22 | 87.34 |
| С | 8.16 | 3.44 | 19.12 | 13.73 | 15.92 | 7.48 |
| 0 | 34.58 | 11.39 | 9.79 | 2.61 | 3.6 | 3.24 |
| Si | 1.76 | 1.03 | 0.46 | 0.16 | 0.18 | 0.33 |
| Cr | 0.45 | 0.98 | 0.51 | 0.28 | 0.23 | 0.23 |
| Mn | 1.02 | 2.58 | 1.88 | 1.23 | 1.08 | 1.23 |
| Мо | 0.85 | 0.01 | 0.13 | 0.06 | 0.07 | 0.16 |
| Cl | 0.04 | 0.01 | 0.04 | nd | nd | nd |
| Others | 0.1 | 1.62 | 0.08 | 0 | 0.69 | 0 |

without and with the inhibitor is 10.24% and 12.38%, respectively, which confirms the presence of organic compounds on the steel surface. At the same time, the iron content is higher in the inhibited sample (82.5% vs. 66.66%), indicating that iron dissolution is hindered on the protected surface. The areas with high iron content may be attributed to cementite (Fe₃C), which becomes exposed after the preferential dissolution of ferrite in the steel microstructure (López et al.,

2003). Reaction products between Fe and CO₂ in an aqueous environment depend on multiple factors, including pH, temperature, exposure time, and the presence of other ions or compounds in the solution. Figure 5 illustrates the changes in the phase composition of corrosion products depending on the Fe-to-CO₂ ratio.

Under conditions where Fe^{2+} coexists with hydroxide (OH⁻) and bicarbonate/carbonate species (HCO_3^-/CO_3^{2-}), coordination complexes of the

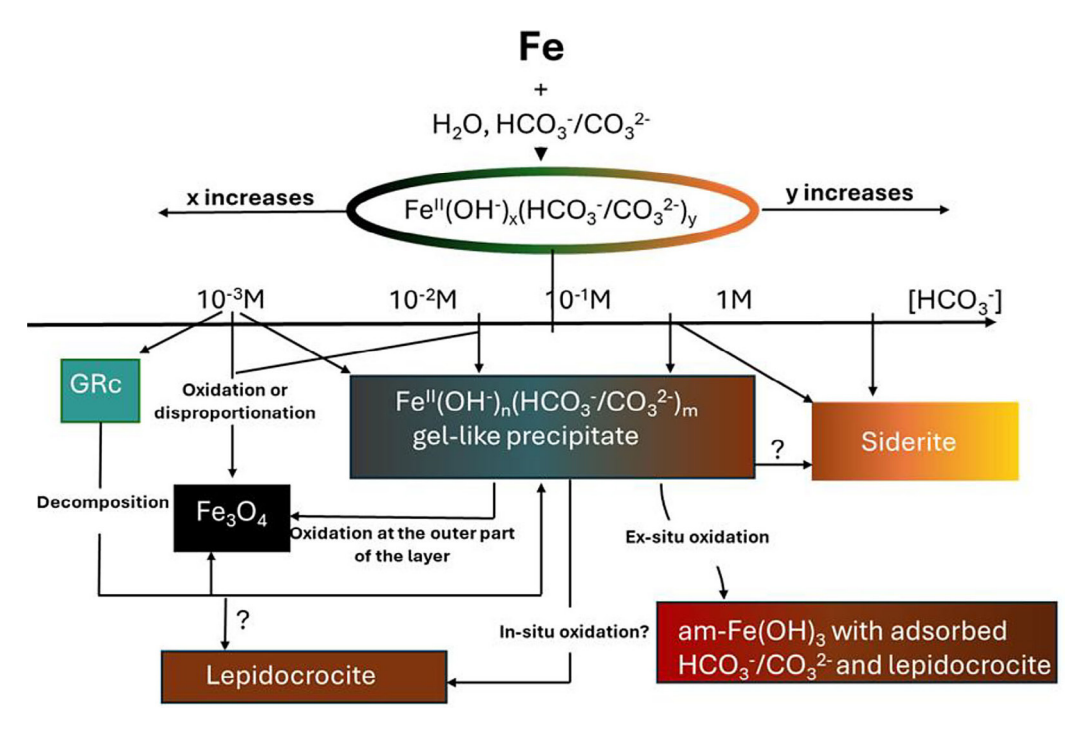


Figure 5. Potential mechanisms for the formation of corrosion products on steel in brine environments rich in carbonates and bicarbonates (adapted from (Savoye et al., 2001))

general formula $Fe^{2+}(OH)_v(HCO_3^-/CO_3^{2-})_v$ are formed (Savoye et al., 2001). As the bicarbonate concentration decreases, the hydroxide content in the complex increases. At elevated bicarbonate levels, transient aqueous species such as FeHCO₃⁺, Fe(HCO₃)₂² and Fe(HCO₃)₂ tend to precipitate as crystalline siderite (FeCO₃). When the HCO₃ concentration falls below approximately 0.1 M, precipitation instead results in a gelatinous amorphous phase. In highly aerated environments, this phase gradually transforms into amorphous ferric hydroxide (Fe(OH)₃), which incorporates adsorbed $C0_3^{2-}$ and $HC0_3^{-}$ ions. Elevated concentrations of dissolved oxygen combined with low bicarbonate levels favor the formation of magnetite (Fe₂O₄). This phase may result from both oxidative pathways and the disproportionation of Fe²⁺(OH)_x(HCO₃⁻/CO₃²⁻)_v complexes. Under the conditions of very low ion concentrations, corrosion products may include green, insoluble Fe(II)-complexes, which, in neutral to mildly alkaline media, can transform into lepidocrocite (γ-FeOOH) and magnetite (Fe₃O₄). Over time, some of these corrosion phases may undergo further transformation: lepidocrocite can convert to goethite (α-FeOOH); goethite and akaganeite (β-FeOOH) can further oxidize to hematite (α-Fe₂O₃); and magnetite may transition to maghemite (γ-Fe₂O₃) (Głuszko, M, 2008).

Under the experimental conditions in this work the concentration of HCO_3^- is at level of few mmol/L with severely limited oxygen availability which leads to the formation of black rust. Visually, black rust appears as a thin, dark film or stain on steel components (Saji, 2019). These darkened regions often become initiation points for localized corrosion, such as pitting, which can further accelerate the degradation process. This form of rust is composed of a dense, compact layer of magnetite (Fe₃O₄) and maghemite (γ-Fe₂O₃) (Klenam et al., 2021). In CO₂-saturated brine, where oxygen levels are low or completely depleted, water functions as the oxidizing agent, facilitating the formation of magnetite while releasing hydrogen gas as a by-product. Due to its thermodynamic stability, black rust can act as a partially protective layer over prolonged exposure periods.

CONCLUSIONS

The present study bridged a knowledge gap concerning the surface chemistry of carbon steel exposed to CO₂-saturated brine at elevated temperature (60 °C) in the presence of a plant-derived corrosion inhibitor. The inhibitor, extracted from mandarin peels, comprises multiple organic constituents bearing hydroxyl, carboxyl,

and ester functionalities, which facilitate physicochemical interactions with the steel surface. Importantly, these compounds remain thermally stable at 60 °C and persist at the metal-solution interface. Scanning electron microscopy (SEM) revealed extensive surface degradation in uninhibited systems after 24 hours of exposure, with the formation of dark corrosion spots and irregular crystallites indicative of localized corrosion processes. Conversely, in the inhibited system, the steel surface exhibited significantly reduced deterioration, with the formation of a uniform, thin, organic layer suggestive of effective surface passivation. EDS analyses enabled qualitative assessment of the corrosion product composition, supporting the proposed inhibition mechanism. On the unprotected surface, the average concentrations of Fe and C were 66.66%, and 10.24%, respectively. In contrast, on the inhibitor-treated surface, these values were 82.5% and 12.38% respectively. The data collectively confirm the efficacy of mandarin peel extract as a thermally stable, eco-friendly corrosion inhibitor capable of mitigating steel degradation in CO₂-rich saline environments.

Acknowledgements

Ewa Knapik acknowledges the support from the Research project "Excellence Initiative – Research University" for the AGH University Grant ID D2 No. 9680 and from AGH University of Krakow (Subsidy No. 16.16.190.779). Przemysław Toczek was supported by the Research project "Excellence Initiative – Research University" at AGH University, Grant ID D1 No. 13984.

REFERENCES

- Al-Janabi, Y. T. (2020). An Overview of Corrosion in Oil and Gas Industry: Upstream, Midstream, and Downstream Sectors. W V. S. Saji & S. A. Umoren (Red.), Corrosion Inhibitors in the Oil and Gas Industry. Wiley-VCH Verlag GmbH & Co. KGaA.
- Bashir, A., Ali, M., Patil, S., Aljawad, M. S., Mahmoud, M., Al-Shehri, D., Hoteit, H., Kamal, M. S. (2024). Comprehensive review of CO₂ geological storage: Exploring principles, mechanisms, and prospects. *Earth-Science Reviews*, 249. https://doi.org/10.1016/j.earscirev.2023.104672
- 3. Błażejowska, M., Czarny, A., Kowalska, I., Michalczewski, A., Stępień, P. (2024). The Effectiveness of the EU ETS Policy in Changing the Energy Mix

- in Selected European Countries. *Energies*, *17*(17). https://doi.org/10.3390/en17174243
- Bouckaert, S., Pales, A. F., McGlade, C., Remme, U., Wanner, B., Varro, L., D'Ambrosio, D., Spencer, T. (2021). Net Zero by 2050: A Roadmap for the Global Energy Sector. International Energy Agency.
- Climate Action Progress Report 2023. (2023). Directorate-General for Climate Action. https://climate.ec.europa.eu/document/download/60a04592-cf1f-4e31-865b-2b5b51b9d09f en
- Dziadzio, P. (2023). CCUS activities in Poland. https://www.energy.gov/sites/default/files/2023-07/5.%20Piotr%20Dziadzio_CCUS%20 activities%20in%20Poland-final.pdf
- Elazabawy, O. E., Attia, E. M., Shawky, N. H., Hyba, A. M. (2023). Eco-friendly orange peel extract as corrosion resistant for carbon steel's deterioration in petroleum formation water. *Scientific Reports*, *13*(1), 21943. https://doi.org/10.1038/ s41598-023-47916-w
- 8. Głuszko, M. (2008). Problems of anticorrosion protection of steel structures and electro energetic equipment exploited in atmospheric conditions. *Prace Instytutu Elektrotechniki*, 235, 1–173.
- Gomez-Guzman, N. B., Martinez de la Escalera, D. M., Porcayo-Calderon, J., Gonzalez-Rodriguez, J. G., Martinez-Gomez, L. (2019). Performance of an amide-based inhibitor derived from coffee bagasse oil as corrosion inhibitor for X70 steel in CO₂-saturated brine. *Green Chemistry Letters and Reviews*, 12(1), 49–60. https://doi.org/10.1080/17518253.2 019.1570352
- Ivanowa, A. (2013). Geological Structure and Time-Lapse Studies of CO₂ Injection at the Ketzin Pilot Site, Germany. Uppsala University.
- 11. Klenam, D. E. P., Bodunrin, M. O., Akromah, S., Gikunoo, E., Andrews, A., McBagonluri, F. (2021). Ferrous materials degradation: Characterisation of rust by colour an overview. 39(4), 297–311. https://doi.org/10.1515/corrrev-2021-0005
- 12. Klimko, R., Hasprová, S. (2025). The Impact of the EU ETS on greenhouse gas emissions in the EU from 2005 to 2022. *Economics and Environment*, 92(1). https://doi.org/10.34659/eis.2025.92.1.874
- 13. Kopacz, M., Matuszewska, D., Olczak, P. (2024). Carbon Capture and Storage (CCS) Implementation as a Method of Reducing Emissions from Coal Thermal Power Plants in Poland. *Energies*, *17*(24). https://doi.org/10.3390/en17246342
- 14. Litvak, O., Litvak, S. (2020). Some aspects of reducing greenhouse gas emissions by using biofuels. *Journal of Ecological Engineering*, 21(8), 198–206. https://doi.org/10.12911/22998993/126967
- López, D. A., Schreiner, W. H., de Sánchez, S. R., Simison, S. N. (2003). The influence of carbon

- steel microstructure on corrosion layers: An XPS and SEM characterization. *Applied Surface Science*, 207(1), 69–85. https://doi.org/10.1016/S0169-4332(02)01218-7
- 16. Łukomska, A., Pulka, J., Broński, M., Dach, J. (2024). Demand-driven biogas plants in Poland Potential and growth perspectives. *Journal of Ecological Engineering*, 25(11), 236–248. https://doi.org/10.12911/22998993/193262
- 17. Ma, Y., Gu, J. (2024). Study on CO₂ corrosion behavior of underground gas storage pipe columns and establishment of corrosion inhibition system. *Processes*, 12(12). https://doi.org/10.3390/pr12122868
- 18. Masuku, C. M., Caulkins, R. S., Siirola, J. J. (2024). Process decarbonization through electrification. *Current Opinion in Chemical Engineering*, 44. https://doi.org/10.1016/j.coche.2024.101011
- 19. Okafor, P. C., Liu, C. B., Liu, X., Zheng, Y. G., Wang, F., Liu, C. Y., Wang, F. (2010). Corrosion inhibition and adsorption behavior of imidazoline salt on N80 carbon steel in CO₂-saturated solutions and its synergism with thiourea. *Journal of Solid State Electrochemistry*, 14(8), 1367–1376. https://doi.org/10.1007/s10008-009-0963-6
- 20. Palumbo, G., Górny, M., Banaś, J. (2019). Corrosion inhibition of pipeline carbon steel (N80) in CO₂-saturated chloride (0.5 M of KCl) solution using gum arabic as a possible environmentally friendly corrosion inhibitor for shale gas industry. *Journal of Materials Engineering and Performance*, 28(10), 6458–6470. https://doi.org/10.1007/s11665-019-04379-3
- 21. Pasieczna-Patkowska, S., Cichy, M., Flieger, J. (2025). Application of Fourier transform infrared (FTIR) spectroscopy in characterization of green synthesized nanoparticles. *Molecules*, *30*(3). https://doi.org/10.3390/molecules30030684
- 22. Prinet, C., Thibeau, S., Lescanne, M., Monne, J. (2013). Lacq-rousse CO₂ capture and storage demonstration pilot: Lessons learnt from two and a half years monitoring. *Energy Procedia*, 37, 3610–3620. https://doi.org/10.1016/j.egypro.2013.06.254
- 23. Pustaj, G., Kapor, F., Jakovljević, S. (2017). Carbon dioxide corrosion of carbon steel and corrosion inhibition by natural olive leaf extract. *Materialwissenschaft und Werkstofftechnik*, 48(2), 122–138. https://doi.org/10.1002/mawe.201600598
- 24. Pustaj, G., Kapor, F., Veinović, Ž. (2016). Olive leaf extract as a corrosion inhibitor of carbon steel in CO₂-saturated chloride–carbonate solution. *International Journal of Electrochemical Science*, 11(9), 7811–7829. https://doi.org/10.20964/2016.09.25
- 25. Saftić, B., Bralić, N., Rukavina, D., Kolenković Močilac, I., Cvetković, M. (2024). Prospects for geological storage of CO₂ in carbonate formations of the Adriatic offshore. *Minerals*, 14(4). https://doi. org/10.3390/min14040409

- 26. Saji, V. S. (2019). Progress in rust converters. *Progress in Organic Coatings*, 127, 88–99. https://doi.org/10.1016/j.porgcoat.2018.11.013
- 27. Sanli, I., Ozkan, G., Şahin-Yeşilçubuk, N. (2025). Green extractions of bioactive compounds from citrus peels and their applications in the food industry. Food Research International, 212, 116352. https://doi.org/10.1016/j.foodres.2025.116352
- Savoye, S., Legrand, L., Sagon, G., Lecomte, S., Chausse, A., Messina, R., Toulhoat, P. (2001). Experimental investigations on iron corrosion products formed in bicarbonate/carbonate-containing solutions at 90 °C. Corrosion Science, 43(11), 2049–2064. https://doi.org/10.1016/S0010-938X(01)00012-9
- Shang, Z., Zhu, J. (2021). Overview on plant extracts as green corrosion inhibitors in the oil and gas fields. *Journal of Materials Research and Technology*, 15, 5078–5094. https://doi.org/10.1016/j.jmrt.2021.10.095
- Shuter, D., Bilio, M., Wilday, J., Murray, L., Whitbread, R. (2011). Safety issues and research priorities for CCS systems and Infrastructure. *Energy Procedia*, 4, 2261– 2268. https://doi.org/10.1016/j.egypro.2011.02.115
- 31. Souza, A. V., da Rocha, J. C., Ponciano Gomes, J. A. C., Palermo, L. C. M., Mansur, C. R. E. (2020). Development and application of a passion fruit seed oil microemulsion as corrosion inhibitor of P110 carbon steel in CO₂-saturated brine. *Colloids and Surfaces A: Physicochemical and Engineering Aspects*, 599, 124934. https://doi.org/10.1016/j. colsurfa.2020.124934
- Stachowicz, A. (2010). Anticorrosive protection with inhibitors for oil and gas production and transportation equipment (in Polish). NAFTA-GAZ, 3, 197–202.
- Stobnicki, P., Gallas, D. (2022). Adoption of modern hydrogen technologies in rail transport. *Journal of Ecological Engineering*, 23(3), 84–91. https://doi. org/10.12911/22998993/145291
- 34. Sun, Z., Singh, A., Xu, X., Chen, S., Liu, W., Lin, Y. (2017). Inhibition effect of pomelo peel extract for N80 steel in 3.5% NaCl saturated with CO₂ solution. *Research on Chemical Intermediates*, 43(11), 6719–6736. https://doi.org/10.1007/s11164-017-3017-1
- 35. Surowska, B. (2002). *Wybrane zagadnienia z koro- zji i ochrony przed korozją*. Wydawnictwo Politechniki Lubelskiej.
- 36. Talus, K., Maddahi, R. (2024). Carbon capture and utilization under EU law: Impermanent storage of CO₂ in products and pre-combustion carbon capture. *The Journal of World Energy Law & Business*, 17(5), 295–308. https://doi.org/10.1093/jwelb/jwae009
- 37. Tang, M., Li, J., Li, Z., Fu, L., Zeng, B., Lv, J. (2019). Mannich base as corrosion inhibitors for N80 steel in a CO₂ saturated solution containing 3 wt % NaCl. *Materials*, 12(3). https://doi.org/10.3390/ma12030449

- 38. Vaca-Cabrero, J., González-Cancelas, N., Camarero-Orive, A., Corral, M. M. E. I., Ricci, S. (2024). Economic impact of the application of the ETS to European ports: Analysis of different scenarios. *Sustainability (Switzerland)*, *16*(23). https://doi.org/10.3390/su162310433
- Vulin, D., Močilac, I. K., Jukić, L., Arnaut, M., Vodopić, F., Saftić, B., Sedlar, D. K., Cvetković, M. (2023). Development of CCUS clusters in Croatia. *International Journal of Greenhouse Gas Control*, 124. https://doi.org/10.1016/j.ijggc.2023.103857
- 40. Wang, H., Tang, J., Xie, J. (2017). Corrosion Inhibition of N80 Steel with the Presence of Asymmetric Gemini in a CO₂-saturated Brine Solution. *International Journal of Electrochemical Science*, 12(11), 11017–11029. https://doi.org/10.20964/2017.11.58
- 41. Wang, S., Wu, B., Qiu, L., Chen, Y., Yuan, J., Chen, S., Bao, M., Fu, C., Wang, X. (2017). Inhibition effect of tangerine peel extract on J55 Steel in CO₂-saturated 3.5 wt. % NaCl Solution. *International Journal of Electrochemical Science*, *12*(12), 11195–11211. https://doi.org/10.20964/2017.12.02
- Wang, S., Zhang, X., Qiu, L., Li, Y., Fu, C. (2017). A kind of corrosion inhibiter containing dried orange peel extracts and its preparation method and application. Patent Appl. No. CN107287600A
- 43. Wang, X., Yang, J., Chen, X., Wang, Y., Yang, Z., Ding, W. (2024). Ecofriendly β-N-butyl amino propionic acid as green corrosion inhibitor for N80 steel in CO₂-saturated brine water. *Journal of Materials Science*, 59(8), 3604–3623 https://doi.org/10.1007/ s10853-024-09375-0
- 44. Wang, X., Yang, J., Chen, X., Yan, K. (2023). Exploring the effectiveness of natural food flavors in

- protecting carbon steel against ${\rm CO}_2$ —induced corrosion. *ACS Omega*, 8(34), 31305–31317. https://doi.org/10.1021/acsomega.3c03762
- 45. Weijermars, R. (2024). Concurrent challenges in practical operations and modeling of geological carbon-dioxide sequestration: Review of the Gorgon project and FluidFlower benchmark study. *Energy Strategy Reviews*, *56*. https://doi.org/10.1016/j.esr.2024.101586
- 46. Wu, R. (2025). Forecasting the European Union allowance price tail risk with the integrated deep belief and mixture density networks. *Chaos, Solitons and Fractals, 199.* https://doi.org/10.1016/j.chaos.2025.116786
- 47. Žbulj, K., Bilić, G., Hrnčević, L., Simon, K. (2021). Potential of using plant extracts as green corrosion inhibitors in the petroleum industry. *Rudarsko-Geološko-Naftni Zbornik*, *36*(5), 132–139. https://doi.org/10.17794/rgn.2021.5.12
- 48. Žbulj, K., Hrnčević, L., Bilić, G., Simon, K. (2022). Dandelion-root extract as green corrosion inhibitor for carbon steel in CO₂-saturated brine solution. *Energies*, *15*(9). https://doi.org/10.3390/en15093074
- 49. Zhang, C., Zhao, J. (2018). Inhibition effects of orange peel extract on the corrosion of Q235 steel in CO₂-saturated and CO₂/H₂S coexistent brine solutions. *Research on Chemical Intermediates*, 44(2), 1275–1293. https://doi.org/10.1007/s11164-017-3166-2
- 50. Zhang, K., Lau, H. C., Chen, Z. (2022). Extension of CO₂ storage life in the Sleipner CCS project by reservoir pressure management. *Journal of Natu*ral Gas Science and Engineering, 108. https://doi. org/10.1016/j.jngse.2022.104814